Verification of polarising optics for the LISA optical bench

Marina Dehne,* Michael Tröbs, Gerhard Heinzel, and Karsten Danzmann

Albert-Einstein-Institute, Max Planck Institute for Gravitational Physics and Leibniz University Hannover, Callinstraße 38, D-30167 Hannover, Germany

marina.dehne@aei.mpg.de

Abstract: The Laser Interferometer Space Antenna (*LISA*) is a space-based interferometric gravitational wave detector. In the current baseline design for the optical bench, the use of polarising optics is foreseen to separate optical beams. Therefore it is important to investigate the influence of polarising components on the interferometer sensitivity and validate that the required picometre stability in the low-frequency band (1 mHz - 1 Hz) is achievable. This paper discusses the design of the experiment and the implemented stabilisation loops. A displacement readout fulfilling the requirement in the whole frequency band is presented. Alternatively, we demonstrate improvement of the noise performance by implementing various algorithms in data post-processing, which leads to an additional robustness for the LISA mission.

OCIS codes: (120.0120) Instrumentation, measurement, and metrology; (120.3180) Interferometry; (230.5440) Polarization-selective devices.

References and links

1. K. Danzmann, T. A. Prince, P. Binetruy, P. Bender, S. Buchman, J. Centrella, M. Cerdonio, N. Cornish, M. Cruise, C. J. Cutler, L. S. Finn, J. Gundlach, C. Hogan, J. Hough, S. A. Hughes, O. Jennrich, P. Jetzer, A. Lobo, P. Madau, Y. Mellier, S. Phinney, D. O. Richstone, B. Schutz, R. Stebbins, T. Sumner, K. Thorne, J.-Y. Vinet, and S. Vitale, "LISA Assessment Study Report," ESA/SRE(2011)3 http://sci.esa.int/science-e/www/object/index.cfm?fobjectid=48364# (2011).
2. K. Danzmann and A. Rüdiger, "LISA technology – concepts, status, prospects," Classical Quant. Grav. **20**, S1–S9 (2003).
3. M. Armano, M. Benedetti, J. Bogenstahl, D. Bortoluzzi, P. Bosetti, N. Brandt, A. Cavalleri, G. Ciani, I. Cristofolini, A. M. Cruise, K. Danzmann, I. Diepholz, G. Dixon, R. Dolesi, J. Fauste, L. Ferraioli, D. Fertin, W. Fichter, M. Freschi, A. Garcia, C. Garcia, A. Grynagier, F. Guzman, E. Fitzsimons, G. Heinzel, M. Hewitson, D. Hollington, J. Hough, M. Hueller, D. Hoyland, O. Jennrich, B. Johlander, C. Killow, A. Lobo, D. Mance, I. Mateos, P. W. McNamara, A. Monsky, D. Nicolini, D. Nicolodi, M. Nofrarias, M. Perreur-Lloyd, E. Plagnol, G. D. Racca, J. Ramos-Castro, D. Robertson, J. Sanjuan, M. O. Schulte, D. N. A. Shaul, M. Smit, L. Stagnaro, F. Steier, T. J. Sumner, N. Tateo, D. Tombolato, G. Vischer, S. Vitale, G. Wanner, H. Ward, S. Waschke, V. Wand, P. Wass, W. J. Weber, T. Ziegler, and P. Zweifel, "LISA Pathfinder: the experiment and the route to LISA," Classical Quant. Grav. **26**, 094001 (2009).
4. G. Heinzel, C. Braxmaier, M. Caldwell, K. Danzmann, F. Draaisma, A. Garcia, J. Hough, O. Jennrich, U. Johann, C. Killow, K. Middleton, M. te Plate, D. Robertson, A. Rüdiger, R. Schilling, F. Steier, V. Wand, and H. Ward, "Successful testing of the LISA Technology Package (LTP) interferometer engineering model," Classical Quant. Grav. **22**, S149–S154 (2005).
5. L. d'Arcio, J. Bogenstahl, M. Dehne, C. Diekmann, E. D. Fitzsimons, R. Fleddermann, E. Granova, G. Heinzel, H. Hogenhuis, C. J. Killow, M. Perreur-Lloyd, J. Pijnenburg, D. I. Robertson, A. Shoda, A. Sohmer, A. Taylor, M. Tröbs, G. Wanner, H. Ward, and D. Weise, "OPTICAL BENCH DEVELOPMENT FOR LISA," in "Proc. of the International Conference on Space Optics, http://congrex.nl/icso/Papers/Session 14b/FCXNL-10A02-2017738-1-weise_icso_paper.pdf," (2010).

#174164 - $15.00 USD Received 10 Aug 2012; revised 22 Oct 2012; accepted 22 Oct 2012; published 20 Nov 2012

6. C.-M. Wu and R. D. Deslattes, "Analytical modeling of the periodic nonlinearity in heterodyne interferometry," Appl. Opt. **37**, 6696–6700 (1998).
7. M. Dehne, M. Sommerfeld, M. Tröbs, G. Heinzel, and K. Danzmann, "Building an ultra-stable optical bench for testing polarising optics in interferometry," presented at 8th LISA symposium, Stanford, USA 28 June - 2 July (2010).
8. M. Dehne, F. G. Cervantes, B. Sheard, G. Heinzel, and K. Danzmann, "Laser interferometer for spaceborne mapping of the Earth's gravity field," JPCS **154**, 012023 (2009).
9. E. J. Elliffe, J. Bogenstahl, A. Deshpande, J. Hough, C. Killow, S. Reid, D. Robertson, S. Rowan, H. Ward, and G. Cagnoli, "Hydroxide-catalysis bonding for stable optical systems for space," Classical Quant. Grav. **22**, S257–S267 (2005).
10. T. J. Kane and R. L. Byer, "Monolithic, unidirectional single-mode Nd:YAG ring laser," Opt. Lett. **10**, 65–67 (1985).
11. S. Anza, M. Armano, E. Balaguer, M. Benedetti, C. Boatella, P. Bosetti, D. Bortoluzzi, N. Brandt, C. Braxmaier, M. Caldwell, L. Carbone, A. Cavalleri, A. Ciccolella, I. Cristofolini, M. Cruise, M. D. Lio, K. Danzmann, D. Desiderio, R. Dolesi, N. Dunbar, W. Fichter, C. Garcia, E. Garcia-Berro, A. F. G. Marin, R. Gerndt, A. Gianolio, D. Giardini, R. Gruenagel, A. Hammesfahr, G. Heinzel, J. Hough, D. Hoyland, M. Hueller, O. Jennrich, U. Johann, S. Kemble, C. Killow, D. Kolbe, M. Landgraf, A. Lobo, V. Lorizzo, D. Mance, K. Middleton, F. Nappo, M. Nofrarias, G. Racca, J. Ramos, D. Robertson, M. Sallusti, M. Sandford, J. Sanjuan, P. Sarra, A. Selig, D. Shaul, D. Smart, M. Smit, L. Stagnaro, T. Sumner, C. Tirabassi, S. Tobin, S. Vitale, V. Wand, H. Ward, W. J. Weber, and P. Zweifel, "The LTP experiment on the LISA Pathfinder mission," Classical Quant. Grav. **22**, S125–S138 (2005).
12. O. Wallner, W. R. Leeb, and P. J. Winzer, "Minimum length of a single-mode fiber spatial filter," J. Opt. Soc. Am. A **19**, 2445–2448 (2002).
13. F. Guzmán Cervantes, "Gravitational wave observation from space: Optical measurement techniques for LISA and LISA Pathfinder," Ph.D. thesis, Leibniz Universität Hannover (2009).
14. G. Heinzel, V. Wand, A. Garcia, O. Jennrich, C. Braxmaier, D. Robertson, K. Middleton, D. Hoyland, A. Rüdiger, R. Schilling, U. Johann, and K. Danzmann, "The LTP interferometer and phasemeter," Classical Quant. Grav. **21**, S581–S587 (2004).
15. M. Tröbs and G. Heinzel, "Improved spectrum estimation from digitized time series on a logarithmic frequency axis," Measurement **39**, 120–129 (2006).
16. M. Tröbs and G. Heinzel, "Corrigendum to "Improved spectrum estimation from digitized time series on a logarithmic frequency axis" [Measurement 39 (2006) 120-129]," Measurement **42**, 170 (2009).
17. V. Wand, J. Bogenstahl, C. Braxmaier, K. Danzmann, A. Garcia, F. Guzman, G. Heinzel, J. Hough, O. Jennrich, C. Killow, D. Robertson, Z. Sodnik, F. Steier, and H. Ward, "Noise sources in the LTP heterodyne interferometer," Classical Quant. Grav. **23**, S159–S167 (2006).
18. R. Fleddermann, F. Steier, M. Tröbs, J. Bogenstahl, C. Killow, G. Heinzel, and K. Danzmann, "Successful demonstration of stray light subtraction in data post-processing for the LISA backlink fiber non-reciprocity experiment," presented at 8th LISA symposium, Stanford, USA 28 June - 2 July (2010).
19. F. Guzman Cervantes, F. Steier, G. Wanner, G. Heinzel, and K. Danzmann, "Subtraction of test mass angular noise in the LISA technology package interferometer," Appl. Phys. B. **90**, 395–400 (2008).
20. "Quartz glass for optics: Data and properties," http://heraeus-quarzglas.com/en/downloads/heraeusquarzglas_1/-downloads.aspx (2011).

1. Introduction

The goal of the Laser Interferometer Space Antenna (*LISA*) is to survey the low-frequency gravitational wave sky (0.1 mHz to 1 Hz) and to detect individual astrophysical sources such as coalescing massive black holes, inspirals of stellar-mass black holes, ultra-compact Galactic binaries and possibly unforeseen sources like relic radiation from the early Universe [1]. In LISA light beams shall propagate between three spacecraft orbiting the Sun in an equilateral triangle constellation of 5 million km side length. The three spacecraft linked by laser light shall act as a Michelson interferometer having a strain sensitivity of $\approx 10^{-20}/\sqrt{\mathrm{Hz}}$ corresponding to optical path length noise of $\approx 10\,\mathrm{pm}/\sqrt{\mathrm{Hz}}$ [2]. Due to the complexity and extreme stability requirements of LISA, a technological precursor mission called LISA Pathfinder (*LPF*) is scheduled and planned for launch in 2014 [3]. It will read out the longitudinal motion and attitude of two free-floating test masses located in one spacecraft with a relative precision in the ten picometre/$\sqrt{\mathrm{Hz}}$ and nanoradian/$\sqrt{\mathrm{Hz}}$ range, respectively [4]. The LISA baseline design foresees a strap-down architecture for measuring the distance fluctuations between the free-floating

#174164 - $15.00 USD Received 10 Aug 2012; revised 22 Oct 2012; accepted 22 Oct 2012; published 20 Nov 2012

test masses: on each satellite, the distance variations between test mass and optical bench are measured and combined with the distance variations between both optical benches. The latter measurement shall be essentially shot-noise limited, the former shall only add negligible noise.

For LISA it is planned to use polarising optics to separate incoming and outgoing beams in the telescope interface and test mass interferometer [5]. The main advantage of this is the possibility to utilise all the light power. Either non-normal incidence on the test mass would have to be used or power would be lost when using a non-polarising beam splitter to separate the beams travelling to and from the test mass. The telescope in LISA is intended to both send and receive light. Here, the power loss would be most severe when using a non-polarising beam splitter to separate incoming and outgoing beam. Possible risks are due to thermal sensitivity of polarising optics which could modify the extinction ratio, the polarising plane as well as the optical path length. Depending on the optical design periodical phase errors can emerge and limit the interferometric sensitivity [6]. As these issues are not present in a non-polarising scheme, an optical layout using non-normal incidence to avoid polarising optics was chosen for LPF. It is therefore of importance to validate that the required $1.42\,\mathrm{pm}/\sqrt{\mathrm{Hz}} \times \sqrt{1+(2.8\mathrm{mHz}/f)^4}$ end-to-end path length stability is achievable with a polarising heterodyne interferometer in the frequency band from 10^{-4} to 1 Hz on the optical bench [5].

An optical bench in a LISA-like setup has been developed to compare the performance of a polarising and a non-polarising interferometer and investigate the behaviour of polarising optics concerning temperature variations and periodic phase errors.

2. Design of the optical bench

The test bench design for investigating the influence of polarising optics on the interferometric sensitivity consisted of four separate heterodyne Mach-Zehnder interferometers on a single stable baseplate. The two measurement interferometers and two auxiliary interferometers were:

1. The *non-polarising interferometer* used only non-polarising elements for relative length measurements. The position fluctuations of mirror M_{TM} was sensed using non-normal incidence as in LPF.

2. The *polarising interferometer* sensed the position fluctuations of the same mirror as in (1) but additionally used polarising optics. The two outputs were compared for relative length measurements.

3. The *reference interferometer* gave a reference phase containing all those environmental noise contributions that were external to the optical bench and common mode in all four interferometers. These fluctuations were subtracted from the polarising and non-polarising interferometers in data post-processing.

4. The *frequency noise interferometer* had an intentional arm length mismatch of about 27 cm and was included for sensing laser frequency noise. Its output signal could be used to actively stabilise the laser frequency or to remove the effect of frequency noise in post-processing.

For a detailed description of the optical layout the reader is kindly referred to references [7, 8].

In each interferometer the number of transmissions through optical components such as beam splitters was equal for both laser beams being used. This minimised the dependency of optical path length on temperature. The beam paths of the two measurement interferometers were designed to occupy roughly the same part on the testbed in order to reduce effects from thermal gradients in the length measurement.

#174164 - $15.00 USD Received 10 Aug 2012; revised 22 Oct 2012; accepted 22 Oct 2012; published 20 Nov 2012

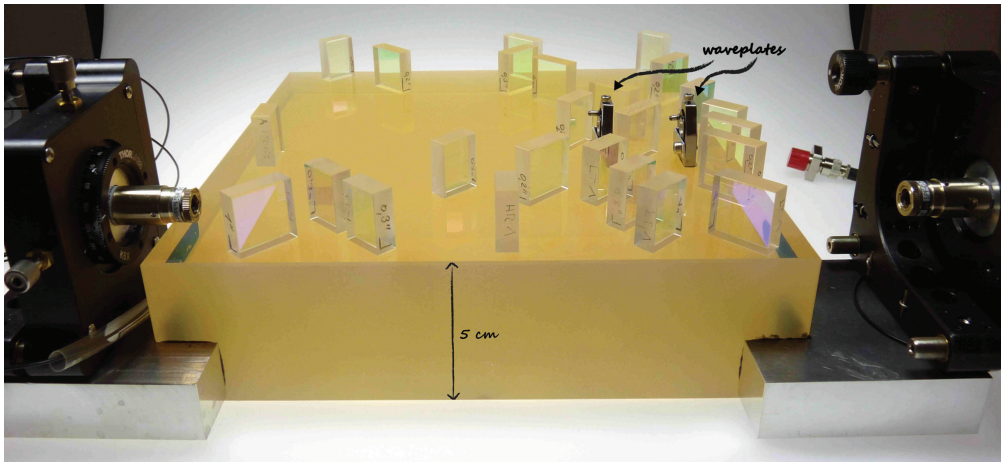

Fig. 1. Final bonded optical bench made of Clearceram® and fused silica components including the glued wave plates and fibre injectors.

In order to achieve high thermal and mechanical stability of the setup all interferometers were combined on a low-expansion glass-ceramic baseplate made of Clearceram® by applying the hydroxide-catalysis bonding technique [9]. A *DEA GLOBAL Advantage* coordinate measuring machine (*CMM*) from Hexagon Metrology GmbH was used to position and align the optical components on the bench. Position accuracies on the order of 10 µm with mean angular deviations of 220 µrad for the component orientation were reached and the two were limited by the CMM accuracy. The achieved arm lengths differences, designed to be nominally zero, were determined to be on the order of 1 mm [7]. A photograph of the final optical bench is shown in Fig. 1.

3. Description of the experimental setup

Earlier experiments of an interferometer including polarising optics had been performed on an aluminium baseplate and a phase readout sensitivity of $1 \times 10^{-2}\,\mathrm{rad}/\sqrt{\mathrm{Hz}}$ that corresponds to $1.7\times10^{-9}\,\mathrm{m}/\sqrt{\mathrm{Hz}}$ longitudinal fluctuations, was reached [8]. The experiences obtained from this setup were used for setting up the new experiment with the quasi-monolithic optical bench.

The final experimental setup is illustrated in Fig. 2. It is divided into two functional parts: the *modulation bench* and the *optical bench*. The modulation bench, which can be seen on the left part, provided the beam preparation and consisted of the laser source and two acousto-optical modulators (*AOMs*). As laser source we used a diode-pumped, monolithic Nd:YAG non-planar ring laser [10] operating at a wavelength of 1064 nm. The linearly polarised single-frequency laser beam was split into two equal parts. Each beam was then shifted in frequency by an AOM driven at approximately 80 MHz, with a frequency difference f_{het} between the two driving signals. A phase-looked loop stabilised the difference frequency between the two AOM drivers to the heterodyne frequency of 1.623 kHz. This modulation scheme is based on the beam preparation for LISA Pathfinder [11]. The two frequency shifted beams were coupled into single mode, polarisation maintaining optical fibres. Those fibres acted as spatial mode-cleaners, which was necessary to achieve high interferometer contrast [12]. The two beams with almost equal optical path length and power were injected into the optical bench containing the four recombiners (RBS_i) and photodiodes. Mirror $\mathrm{M_{TM}}$ was read out by a polarising interferometer ($\mathrm{RBS_p}$) and

#174164 - $15.00 USD Received 10 Aug 2012; revised 22 Oct 2012; accepted 22 Oct 2012; published 20 Nov 2012

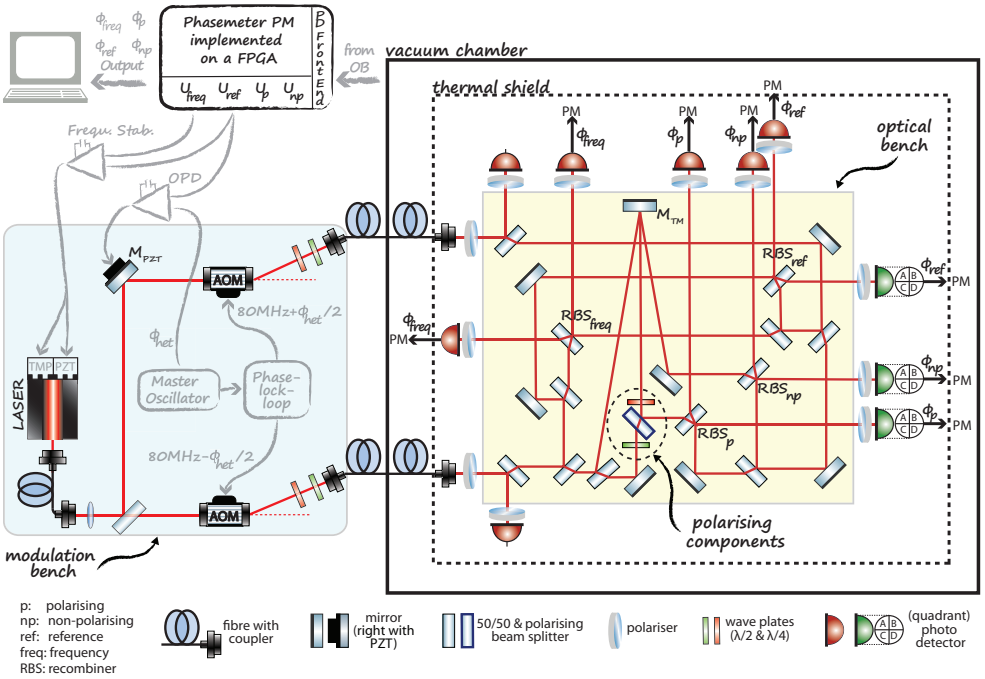

Fig. 2. Schematic of the experimental setup. *Left*: the modulation bench provides the beam preparation. *Right*: the optical bench containing the interferometers enclosed by a thermal shield inside a vacuum chamber. The implemented stabilisation loops are greyed out.

a non-polarising interferometer (RBS_{np}). Along with the 8 single element photodiodes three quadrant photodiodes were implemented for differential wavefront sensing (*DWS*) [13]. The obtained phases ϕ_i (i ={ p, np, ref, freq}) were measured with a hardware phase meter, implemented using field-programmable gate arrays (*FPGAs*) [14].
The following sections describe the efforts made to reduce external influences on the noise performance.

3.1. Reduction of environmental influences

Fluctuations in air pressure lead to fluctuations in the refractive index of air and appear as path length changes. In order to avoid coupling of this noise source and thermal effects into the phase readout, the measurement was conducted in vacuum. For a further reduction of temperature noise a thermal shield (*TS*) was used, which consisted of an aluminium baseplate on ceramic spacers made of Macor® with a cover made of polished aluminium sheet metal. It acted as a thermal low-pass and reduced the heat conduction and heat radiation. In order to verify the impact of the thermal shield on the temperature noise the temperature was measured at different locations in the vacuum chamber as well as inside the thermal shield. The resulting noise estimates indicated a suppression of more than four orders of magnitude compared to room temperature as depicted in Fig. 3. The lpsd algorithm [15, 16] was used for this and all other spectral estimates in this paper. Measurements conducted inside the chamber were limited by the sensor noise for frequencies above 2 mHz. As temperature sensors we used platinum resistors (PT10000).

In order to reduce vibrations induced by the pump system we used a passive vibration isola-

#174164 - $15.00 USD Received 10 Aug 2012; revised 22 Oct 2012; accepted 22 Oct 2012; published 20 Nov 2012

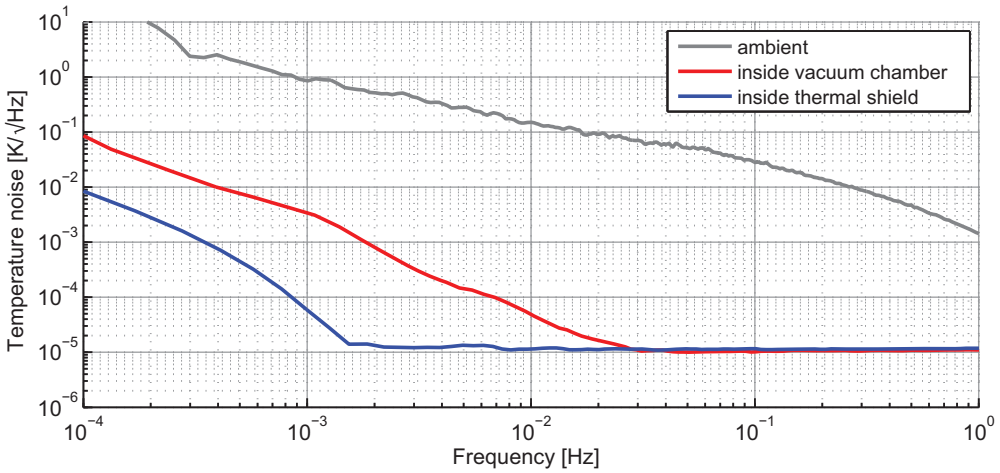

Fig. 3. Measured temperature noise in- and outside the vacuum chamber to verify the effect of the thermal shield.

tion of the optical table with the vacuum chamber on it, as shown in Fig. 4. The pump system is located under the chamber and isolated via a diaphragm bellows. Vacuum compatible dampers were installed under the thermal shield. This led to a vibration isolation for excitation frequencies above 10 mHz.

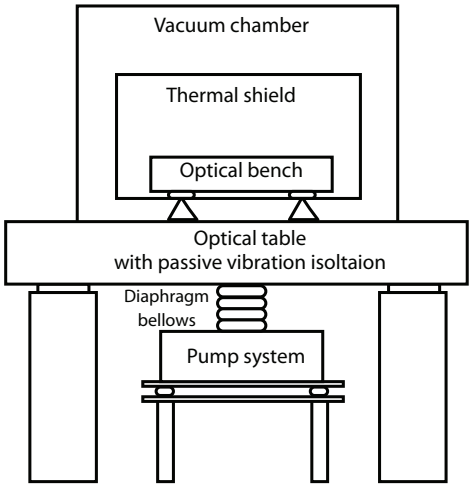

Fig. 4. Schematic of the setup to reduce environmental influences: the vacuum system is places on an optical table with passive vibration isolation, whilst the pump system is located under the optical table and isolated via a diaphragm bellows. A thermal shield inside the chamber isolates the optical bench from temperature fluctuations.

#174164 - $15.00 USD Received 10 Aug 2012; revised 22 Oct 2012; accepted 22 Oct 2012; published 20 Nov 2012

3.2. Optical path length difference stabilisation

The interferometer concept included a reference interferometer which sensed common-mode phase fluctuations caused by environmental noise, such as fluctuations in the unstable modulation bench. By subtracting this reference phase from the measurement phases, these fluctuations canceled for frequencies less than 1 Hz.

Electrically induced sidebands on the light, which give rise to non-linearities in the interferometer output, can reduce this common mode noise rejection and disturb the interferometer sensitivity [17]. In order to mitigate this periodic phase error, a stabilisation of the optical path length difference (*OPD*) has been implemented by comparing the reference phase ϕ_{ref} to the electronic phase ϕ_{het} of the reference oscillator. The phase difference was held constant in closed-loop control by actuating mirror $\mathrm{M_{PZT}}$ on the modulation bench that is mounted on a piezoelectric element.

3.3. Control of the polarisation state stability

In worst case, a non-matching polarisation state of the beam relative to the fibre axis would lead to a circular polarised light, changing in response to external influences on the fibre resulting in laser power fluctuations. In addition, residual interference with the wrong polarisation can induce a parasitic noise in the phase readout. By enhancing the polarisation state stability such noise sources were suppressed.

To ensure a stable s-polarisation state on the optical bench, Glan-Thompson polarisers were installed at both fibre outputs on the optical bench. Additionally, two retardation plates ($\lambda/2$ and $\lambda/4$) were placed in front of the fibre inputs. With these it was possible to match the input polarisation state to the polarisation-maintaining axes of the fibres, which were monitored with a polarimeter (*SK9782-NIR*, Schäfter & Kirchhoff). Thin-film polarisers (*colorPol® VISIR CW02*, Codixx) with an extinction ratio of 10^6 were placed directly in front of each photodiode. The photodiodes were tilted by a few degrees to avoid ghost reflections back into the optical setup.

3.4. Impact of frequency noise on longitudinal phase noise

In a heterodyne interferometer the path length difference ΔL between the two interfering beams translates into phase fluctuations $\widetilde{\delta\phi}$ at the heterodyne frequency. The translation of frequency noise $\widetilde{\delta\nu}$ into phase noise is given by the differential time delay $\Delta L/c$ as

$$\widetilde{\delta\phi} = \frac{\Delta L}{c} 2\pi \widetilde{\delta\nu}, \tag{1}$$

where c is the speed of light.

Path length differences before the optical bench cancel by referring all measurements to the reference interferometer and only those on the optical bench couple into the phase measurement. By intentionally modulating the laser frequency as described in Section 4.3 below, we measured arm length differences of 1.5 mm and 500 μm for the non-polarising and polarising interferometer, respectively. For the phase fluctuations to remain below 8.4 μrad/$\sqrt{\mathrm{Hz}}$ corresponding to path length fluctuations of 1.42 μm/$\sqrt{\mathrm{Hz}}$, the required frequency stability for both measurement interferometers can be calculated to:

$$\widetilde{\delta\nu}_{\mathrm{np}} = 267 \frac{\mathrm{kHz}}{\sqrt{\mathrm{Hz}}} \left[\frac{1.5\,\mathrm{mm}}{\Delta L}\right] \qquad \widetilde{\delta\nu}_{\mathrm{p}} = 802 \frac{\mathrm{kHz}}{\sqrt{\mathrm{Hz}}} \left[\frac{0.5\,\mathrm{mm}}{\Delta L}\right]. \tag{2}$$

The measured free-running frequency noise of the unstabilised Nd:YAG NPRO laser (used in the experimental setup) at 10 mHz is about 2×10^6 Hz/$\sqrt{\mathrm{Hz}}$ and is depicted in Fig. 5 by the red

#174164 - $15.00 USD Received 10 Aug 2012; revised 22 Oct 2012; accepted 22 Oct 2012; published 20 Nov 2012

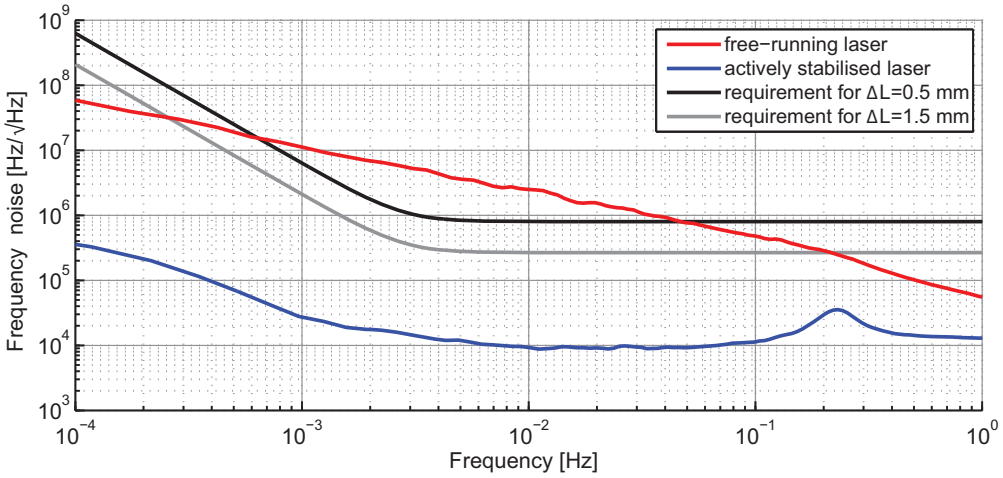

Fig. 5. Measured laser frequency noise in free-running and stabilised condition; the red trace shows the free-running noise, the blue trace shows the remaining noise obtained from the in-loop error signal when the laser frequency was stabilised; the black and grey traces show the requirements on laser frequency noise for 0.5 mm and 1.5 mm interferometer path length difference.

trace. This has been determined by using Eq. (1) together with the measured longitudinal signal using the auxiliary interferometer with an intentionally arm length mismatch of $\Delta L = 27.4$ cm. As a result, the frequency fluctuations of a free running laser would be a significant noise source in the two measurement interferometers. For that reason the auxiliary interferometer (iv) was used to sense the laser frequency fluctuations. Using a feedback loop the laser frequency was actively stabilised. We used an analogue servo containing two input channels for the photodiode signals of the reference and frequency interferometers. With an analogue multiplier the phase difference between both signals was determined. In order to suppress the heterodyne frequency and its harmonics the signal was low-pass filtered. This error signal was converted into two different feedback signals. The first one was fed to the piezoelectric-based fast laser frequency actuation and the second feedback signal for the slower laser crystal temperature tuning. The bandwidth of the control loop achieved was about 3 Hz (increasing with $1/f$ towards lower frequencies).

A laser frequency stability of $10\,\mathrm{kHz}/\sqrt{\mathrm{Hz}}@\,10\,\mathrm{mHz}$ was achieved as illustrated in Fig. 5 along with the required stability for the two measurement interferometers (*cf.* Eq. (2)). For estimating the achieved stability the signal measured with the auxiliary interferometer and the determined arm length difference were fed in Eq. (1). We reached a stability improvement in frequency noise of more then two orders of magnitude for frequencies smaller then 100 mHz. We believe the stability was limited by electronic noise in the photodiodes, multiplier and low-pass filter. Although this "in-loop" measurement can only give a lower limit for the real frequency noise, the later results confirm that the frequency noise suppression was sufficient for this experiment. The feature at 0.25 Hz in the blue trace is possibly due to a crossover between two actuators in the frequency stabilization: the fast PZT loop and the outer slower loop acting on the laser crystal temperature.

#174164 - $15.00 USD Received 10 Aug 2012; revised 22 Oct 2012; accepted 22 Oct 2012; published 20 Nov 2012

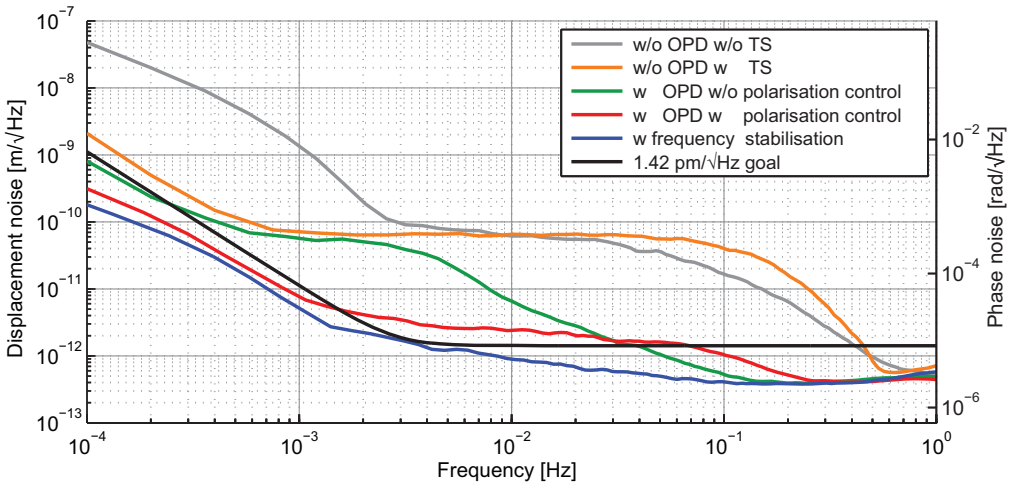

Fig. 6. Displacement noise of the polarising interferometer while different stabilisations were implemented (*w*: with, *w/o*: without, *OPD*: optical path difference stabilisation, *TS*: thermal shield); all measurements were conducted in vacuum.

3.5. Noise performance

The noise performance of the polarising interferometer is shown in Fig. 6 together with its requirement. The grey trace displays the initial measurement conducted in a vacuum environment ($\approx 10^{-6}$ mbar) without any stabilisations and without thermal shield. A significant improvement for frequencies ≤ 3 mHz was obtained by enclosing the optical bench with a thermal shield (orange trace). The noise shoulder is a sign of periodic phase errors. Therefore an OPD stabilisation was adopted and led to a significant improvement of the displacement noise for frequencies above 3 mHz (green trace). By equipping the optical bench with polarisers and controlling the incoming polarisation state of the two beams, the phase readout noise was reduced in the frequency band between 0.3 and 30 mHz (red trace). Afterwards a stabilisation loop of the laser's frequency was applied. The final displacement noise (blue trace) was below the requirement in the whole frequency range.

4. Noise subtraction in data post-processing

So far the external influences impairing the noise performance have been identified. For a successful mitigation, different stabilisation schemes were presented. Yet another possibility for improving the phase readout is to eliminate noise sources in the data post-processing. In the following the subtraction models used are presented.

4.1. Subtraction of spurious beat note signals

As spurious beat note signals can significantly impair the phase readout, a careful design concerning stray light is mandatory. The rear side of each optical component, even if equipped with an anti-reflective coating, generates ghost beams, which may eventually reach the detector. Although the bench has been designed such as to minimise their effect, some ghost beams can not be avoided. They are sharing the same optical path and beam parameters as the main laser beam. Two kinds of spurious beat note signals can be distinguished: *i*) those where a ghost beam interferes with a main beam at the recombination beam splitter and *ii*) those where a ghost beam interferes prior to the recombination beam splitter. The nominal beat signal will

#174164 - $15.00 USD Received 10 Aug 2012; revised 22 Oct 2012; accepted 22 Oct 2012; published 20 Nov 2012

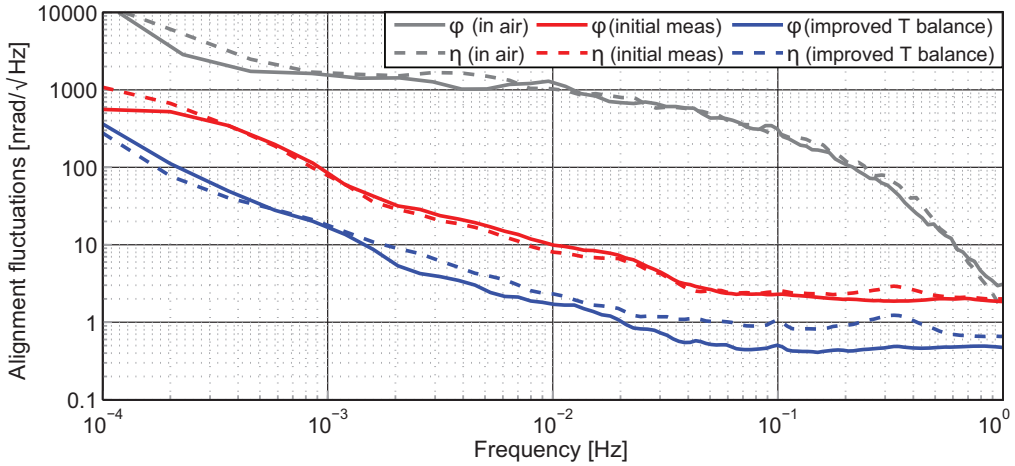

Fig. 7. Angular noise of a measurement in air but enclosed by the vacuum chamber (grey) along with one conducted for a few days in the evacuated chamber (blue) and after reaching a state close to thermal equilibrium (red).

leave the two recombiner ports with a phase difference of 180 ° due the conservation of energy. In case *i*) the interference signal between ghost beam and main beam also show 180 ° phase difference. Hence, they cannot be distinguished from the nominal signal. In case *ii*) however the phase difference between ghost beam and nominal beam is 0 °. This parasitic signal cancels if the difference of both interference signals is taken, which at the same time doubles the main signal.

By applying this correction in the data post-processing it is important to normalise the signals with respect to the measured amplitude, which also includes the stray light part [18]. This correction scheme was used for a post measurement subtraction of stray light in all measurement interferometers. However, no noise subtraction has been performed in data post processing to produce Fig. 6.

4.2. Angular noise subtraction

It is necessary to monitor the fibre injectors attitude jitter in order to characterise a cross-coupling between angular and displacement degrees of freedom. For this reason, the optical bench included quadrant photodiodes (QPD) at the three main interferometer outputs. In the post measurement correction the differential wavefront sensing (*DWS*) technique has been applied [19]. It starts with a separate phase measurement on each segment of the quadrant photodiode. The horizontal DWS signal φ was calculated from the phase difference between the left and the right side of one QPD. Thus, a signal results which depends on the relative angle between the wavefronts of the two interfering beams. In the same manner, the vertical wavefront tilt η was obtained from the phase difference between the upper and the lower quadrants of the same QPD. For specifying the angular noise the coupling factor of DWS signal [phase change in rad] to beam angle change has been determined. This was done by introducing well defined beam angle changes and monitoring the resulting changes in DWS signals. The coefficients obtained were calculated to be approximately 3800 rad/rad. The angular noise is caused by temperature and air fluctuations, as depicted in Fig. 7. The grey traces show the angular noise for measurements in the non-evacuated vacuum chamber. The blue traces belong to the measurement shown in Fig. 8 (green trace) for demonstrating the different subtraction algo-

#174164 - $15.00 USD Received 10 Aug 2012; revised 22 Oct 2012; accepted 22 Oct 2012; published 20 Nov 2012

rithms. This measurement was taken a few days after the chamber was closed and evacuated whereas the red traces show the measurement taken two weeks after the chamber was closed and evacuated. The temperature stability had reached an equilibrium while the pressure stayed at a constant level.

To estimate the influence of angular noise on length change MATLAB©'s built-in least squares fit method was used. Band-pass filtered angular and longitudinal interferometric signals were fed to the fit algorithm [19]. Typically corner frequencies were 1 mHz and 100 mHz, between which the longitudinal and angular signals were influenced by the assigned noise source. The coefficients obtained were used to subtract the spurious noise from the stray light corrected longitudinal signal.

4.3. Frequency noise subtraction

The second auxiliary interferometer with unequal arm length provides a frequency fluctuation signal ϕ_{freq}. This signal was used in an active stabilisation loop as described in Section 3.4. Alternatively it can be used in a post-measurement correction. For this reason the frequency coupling coefficients corresponding to the arm length imbalances were determined. This was done by modulating the laser frequency, while observing the resulting coupling to the interferometric phase, where they appear scaled by the arm length difference of each interferometer, as given by Eq. (1). The resulting ratio c_m of the modulation peak height δ, expressed by

$$c_m = \frac{\delta(\phi_m - \phi_{\mathrm{ref}})}{\delta(\phi_{\mathrm{freq}} - \phi_{\mathrm{ref}})}, \tag{3}$$

were used for long-term measurements to obtain a frequency noise corrected interferometric phase as

$$\Psi_{\mathrm{cor}} = (\phi_m - \phi_{\mathrm{ref}})_{\mathrm{SL/DWS}} - c_m \cdot (\phi_{\mathrm{freq}} - \phi_{\mathrm{ref}})_{\mathrm{SL/DWS}}, \tag{4}$$

where the stray light (*SL*) and angular noise (*DWS*) subtractions were adopted earlier.

4.4. Temperature noise subtraction

The noise performance in the low frequency range (≤ 1 mHz) was dominated by temperature noise. Although we have placed the optical bench in a vacuum environment, enclosed it by a thermal shield and used low-expansion ceramic as material for the optical bench, the temperature influenced the stability at the pm/$\sqrt{\mathrm{Hz}}$ level. Therefore the measured temperature inside the thermal shield was used in a linear fit for estimating a coefficient between temperature and measured phase. By using again a least squares fit method implemented in MATLAB© the coefficient was determined to be about 1.3 rad/K. Using this coefficient the temperature induced phase changes where subtracted from the main measurement. Note that we were not limited by temperature variations if we enclosed the bench for more than one week. An adequate state close to the thermal equilibrium ($\widetilde{\delta T} \leq 1\mathrm{mK}/\sqrt{\mathrm{Hz}}$@1 mHz) was reached after one week, further improving with longer setting time.

Coupling factor between temperature of PBS and longitudinal phase signal

The influence of temperature fluctuations at the polarising components, in particular the PBS, to the longitudinal phase has been investigated. The PBS used was made of fused silica with a dielectric coating. Any modifications of the extinction ratio or polarisation plane result in power fluctuations, which couple to the longitudinal measurement. Therefore, the PBS was heated up with a Kapton™ heater (*HK 5186*, MINCO) while the temperature at the beam splitter and the corresponding phase was monitored. In order to measure only induced phase changes of the PBS, the phase difference of the two main interferometers was used.

#174164 - $15.00 USD Received 10 Aug 2012; revised 22 Oct 2012; accepted 22 Oct 2012; published 20 Nov 2012

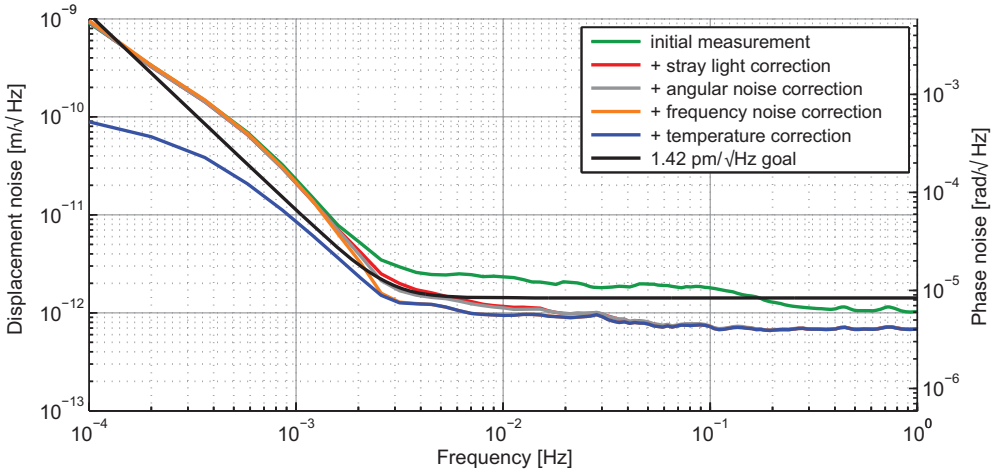

Fig. 8. Displacement noise of the p-interferometer to show the effect of data post-processing: *Green*: initial measurement with OPD stabilisation and polarisation control in vacuum, *Red*: with stray light correction, *Grey*: with angular noise correction, *Orange*: with frequency noise correction and *Blue*: with temperature noise correction.

By considering a single pass through the PBS and the influence of the reflection at the return path, the coupling of temperature change dT to the optical path length change ds by the PBS can be expressed by

$$\frac{\mathrm{d}s}{\mathrm{d}T} = \underbrace{\frac{\mathrm{L}}{\sqrt{1-\left(\frac{\sin\theta}{n}\right)^2}}\left[\frac{\mathrm{d}n}{\mathrm{d}T}\left(1-\frac{\sin^2\theta}{n(n^2-\sin^2\theta)}(n-1)\right)+\alpha(n-1)\right]}_{\text{single pass through PBS}} - \underbrace{\frac{\alpha \mathrm{L}}{\sqrt{2}}}_{\text{reflection}}, \tag{5}$$

where θ is the angle of incidence (= 45°). The thermal expansion coefficient α is 0.51 ppm/K and the refractive index n of fused silica at 1064 nm is 1.44963 [20]. With a temperature coefficient of the refractive index dn/dT of 9.8 ppm/K [20] we can estimate a coupling coefficient proportional to the geometric thickness L (≈7 mm) of the PBS of 10 ppm/K. To compare the results obtained from heating the PBS we can express the coupling of temperature to the optical path length in terms of phase in single pass (including the reflection on the optical surface of the PBS) by

$$\frac{\mathrm{d}\Phi}{\mathrm{d}T} = \frac{2\pi}{\lambda}\frac{\mathrm{d}s}{\mathrm{d}T} \approx 0.4\,\frac{\mathrm{rad}}{\mathrm{K}}. \tag{6}$$

The experimentally determined coupling coefficient of 0.3 rad/K roughly agrees with the theoretical value. The discrepancy can be caused by having not measured the temperature inside the PBS, but on the optic's surface. However, a temperature stability in the polarising beam splitter required to detect path length fluctuations of $1\,\mathrm{pm}/\sqrt{\mathrm{Hz}}$ is thus approximately $2\cdot10^{-5}\,\mathrm{K}/\sqrt{\mathrm{Hz}}$. Using the coupling coefficient of 1.3 rad/K for the interferometer including all components an over all temperature stability requirement of $4.5\,\mu\mathrm{K}/\sqrt{\mathrm{Hz}}$ for frequencies smaller than 3 mHz can be deduced.

4.5. Noise performance

The displacement noise with implemented noise subtraction models are presented in Fig. 8. The initial measurement is a length measurement of the polarising interferometer conducted

#174164 - $15.00 USD Received 10 Aug 2012; revised 22 Oct 2012; accepted 22 Oct 2012; published 20 Nov 2012

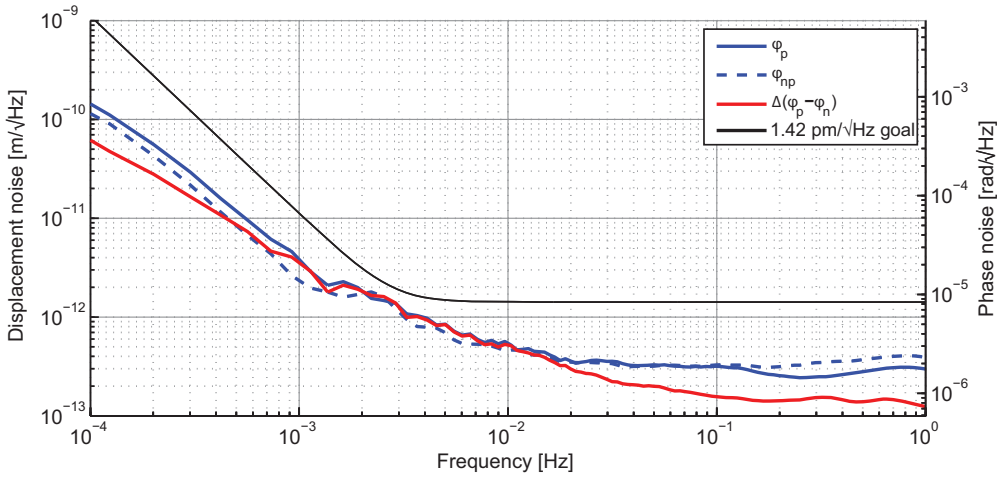

Fig. 9. Displacement noise of the two measurement interferometers in the final setup along with their difference.

for a few days in a vacuum environment while it was enclosed by a TS (green trace). The OPD stabilisation was used and the polarisation state of the two beams injected to the bench were controlled. Residual noise induced by stray light was eliminated by balanced detection. The correction applied led to a considerable reduction of the displacement noise observed for frequencies bigger than 2 mHz (red trace). The grey trace illustrates the displacement noise with an additional angular noise subtraction. This subtraction only improves the phase readout in the small frequency band from 2 mHz to 20 mHz. By implementing the frequency noise subtraction algorithm we obtained a displacement sensitivity well below the requirements for frequencies bigger than 2 mHz (orange trace). For frequencies smaller than 2 mHz we were limited by temperature noise. However, we were able to notably enhance the phase readout sensitivity by applying a temperature noise subtraction. Thus, the blue trace represents the final displacement sensitivity, where all the noise subtractions presented were applied. One can see that the noise performance fulfils the requirement in the whole frequency range.

By combining the subtraction algorithms with the stabilisation loops the performance could be enhanced. Figure 9 depicts the noise performance for the two measurement interferometers ($\phi_\mathrm{p}, \phi_\mathrm{np}$) along with the difference between these two signals $\Delta(\phi_\mathrm{p} - \phi_\mathrm{np})$. For this measurement we used the OPD stabilisation (Sec. 3.2) as well as a frequency stabilisation and matched the polarisation state of the two beams to the optical fibres. A stray light correction as well as an angular and temperature noise subtraction were implemented in the data post-processing. The noise traces obtained fulfil the requirement within the whole frequency band. Furthermore, the noise of the difference between polarising and non-polarising interferometer complies with the required 1.42 pm/$\sqrt{\mathrm{Hz}}$ level.

Nevertheless, noise subtraction techniques have to be performed very carefully and the results obtained have to be critically evaluated, as there is a non-vanishing probability to corrupt the data. However, as it can be seen in Fig. 8, the corrected data reached the same level of the measurements performed with actively stabilisations (*cf.* Fig. 6), which indicates that the several cross-coupling effects, e.g. from frequency fluctuations into the longitudinal signal, has been fitted and subtracted without corrupting the data. The determined coupling coefficients can be differ from the true values resulting in a non-perfect extracting of the noise source. Thus, the results obtained indicate only an upper limit of the noise performance.

#174164 - $15.00 USD Received 10 Aug 2012; revised 22 Oct 2012; accepted 22 Oct 2012; published 20 Nov 2012

5. Periodic phase errors

In heterodyne interferometry the sensitivity can be limited by non-linear effects. While a number of different sources for those effects exist, they all share the same principle: A parasitic interference signal is generated, that is detected together with the nominal signal and adds to it. While the phase of the nominal signal may be constant, a change of phase or amplitude of the parasitic signal can alter the phase of the combined signal. In our setup, such non-linear errors are known to be induced by spurious sidebands on the AOM radio frequency driving signals [17]. They have been mitigated through an optical path length stabilisation as discussed in Sec. 3.2.

By using polarising optics in heterodyne interferometry additional sources for periodical phase errors emerge depending on the setup. These can be among others elliptically polarised laser beams, beam splitter leakage and rotational errors in the alignment of laser and polarisation beam splitter or retardation plates [6]. Through frequency or polarisation mixing they can induce a spurious beat note signal. Since after analysing our heterodyne scheme no cross-talk between the two main beams and residual beams emerging from the sources mentioned is apparent, we do not expect periodic phase errors caused by polarising components. In order to verify our assumption we modified our setup to be able to induce path length changes in one arm of the two measurement interferometers. By "replacing" the 0°-mirror (mirror M_{TM} in Fig. 2) with a piezo-actuated mirror the path length was changed by around 5 µm for both, polarising and non-polarising interferometers, consecutively. The measured displacement of the two interferometers were compared to the induced displacement that was obtained from the voltage applied to the piezo. The displacement in the polarising interferometer is plotted in Fig. 10.

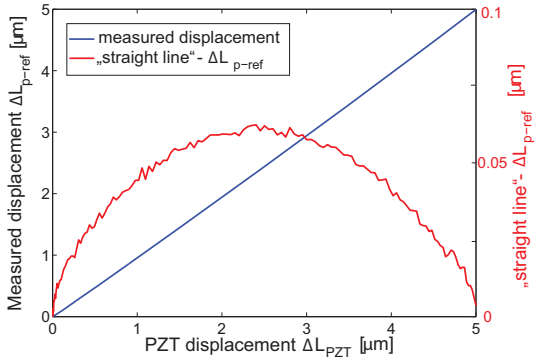

Fig. 10. The measured displacement of the polarising interferometer ΔL_{p-ref} versus the displacement of the piezoelectric element (PZT). The solid red line represents the deviation of measured data to a straight line.

In an ideal case the PZT modulation would result in a linear length variation. However, if the polarising components induce a non-linear effect, we would expect to see five cycles for first-harmonic non-linearity and ten cycles for second-harmonic non-linearity, as five fringes were scanned. Non-linearities caused by polarising optics are not present but rather the curve shape can be interpreted as the non-linearity of the piezo-actuated mirror. This is also confirmed by the difference of measured and theoretic displacement deviating from zero (red trace).

#174164 - $15.00 USD Received 10 Aug 2012; revised 22 Oct 2012; accepted 22 Oct 2012; published 20 Nov 2012

6. Conclusions

Displacement noise below 1.42 pm/$\sqrt{\text{Hz}}$ was demonstrated in a heterodyne interferometer using polarising components.

For this purpose a quasi-monolithic optical bench was built by applying the hydroxide-catalysis bonding technique. The bonded setup consisted of two measurement interferometers (one including polarising components) and two auxiliary interferometers. One of them had unequal arm lengths and was used to actively stabilise the laser's frequency to 10 kHz/$\sqrt{\text{Hz}}$ @ 10 mHz. Length measurements for the polarising and non-polarising interferometer were compared and found to be below 1.42 pm/$\sqrt{\text{Hz}}$ in the frequency band from 3 mHz to 1 Hz relaxing towards lower frequencies. In order to reach that noise level different noise sources were identified and suppressed. Alternatively, they were subtracted in data post-processing. These noise sources were parasitic beams due to ghost reflections (stray light) and coupling of noise into the displacement measurement such as beam angle noise, temperature noise, and laser frequency noise. Thus, under non-ideal conditions it was still possible to reach the required noise performance, which leads to an improved robustness for a LISA mission. The requirements for frequency noise, temperature noise and geometric beam jitter in the LISA mission are more strict than the values used in the experiment. We have demonstrated performance as required in LISA under worse conditions than currently anticipated for LISA. The measured coupling from the temperature of the polarising optics to the displacement measurement was as expected. No evidence was found for periodic phase errors induced by polarising optics.

Acknowledgments

We acknowledge funding by the European Space Agency within the project "Optical Bench Development for LISA", and support by Deutsches Zentrum für Luft und Raumfahrt (DLR) with funding from the Bundesministerium für Wirtschaft und Technologie (DLR project reference 50 OQ 0601). We thank the German Research Foundation for funding the cluster of Excellence QUEST - Centre for Quantum Engineering and Space-Time Research.

#174164 - $15.00 USD Received 10 Aug 2012; revised 22 Oct 2012; accepted 22 Oct 2012; published 20 Nov 2012